Available online at www.sciencedirect.com

SciVerse ScienceDirect

Scripta Materialia 69 (2013) 424–427

Scripta MATERIALIA

www.elsevier.com/locate/scriptamat

Influence of supersaturated carbon on the diffusion of Ni in ferrite determined by atom probe tomography

T. Kresse,[a] Y.J. Li,[b] T. Boll,[c] C. Borchers,[a] P. Choi,[b] T. Al-Kassab,[c] D. Raabe[b] and R. Kirchheim[a,b,d,*]

[a]*Institut für Materialphysik, Georg-August-Universität Göttingen, Friedrich-Hund-Platz 1, D-37077 Göttingen, Germany*
[b]*Max-Planck-Institut für Eisenforschung, Max-Planck-Strasse 1, D-40237 Düsseldorf, Germany*
[c]*Division of Physical Science and Engineering, King Abdullah University of Science and Technology, Thuwal 23955-6900, Saudi Arabia*
[d]*International Institute for Carbon-Neutral Energy Research (WPI-I2CNER), Kyushu University, Japan*

Received 2 May 2013; accepted 29 May 2013
Available online 5 June 2013

In patented and cold-drawn pearlitic steel wires dissociation of cementite occurs during mechanical deformation. In this study the influence of the carbon decomposition on the diffusion of nickel in ferrite is investigated by means of atom probe tomography. In the temperature range 423–523 K we observed a much smaller activation energy of Ni diffusion than for self-diffusion in body-centered cubic iron, indicating an increased vacancy density owing to enhanced formation of vacancy–carbon complexes.

Keywords: Vacancy–carbon complexes; Ni diffusion, Self-diffusion; Face-centered cubic iron; Body-centered cubic iron; Atom probe tomography

Previous studies on diffusion in metal/carbon alloys showed an increase in the diffusion coefficient $D = D_0 \exp(-Q/k_B T)$ (with prefactor D_0, activation enthalpy Q and temperature T) for self-diffusion in face-centered cubic (fcc) iron [1], self-diffusion in hexagonal close-packed Co [2] and Co diffusion in Ni [2,3] on increasing the solute carbon content in the material. This was interpreted as an enlarged vacancy concentration compared with the equilibrium value due to the formation of vacancy carbon complexes. However, theoretical studies for body-centered cubic (bcc) iron showed a decrease in self-diffusion in the presence of carbon [4,5] interpreted as decreased mobility of vacancy–carbon complexes. In the present study nickel diffusion coefficients in the carbon containing ferrite lamellae of pearlitic steel were determined using atom probe tomography (APT), in order to determine whether Ni diffusivity is increased, like measured self-diffusion in fcc iron, or decreased, as predicted for self-diffusion in bcc iron. Nickel was chosen as the diffusing element in ferrite because its activation enthalpy for diffusion in bcc iron (2.55 eV [6]) is similar to the activation enthalpy of iron self-diffusion (2.60 eV [7]). APT yields three-dimensional elemental maps at near-atomic resolution. Such data enable us to calculate diffusion coefficients from nickel concentration profiles extending over only a few nanometers occurring at low annealing temperatures.

Deformed pearlitic wires were chosen because previous APT measurements have shown that their ferrite lamellae contain carbon well above the equilibrium value of bcc iron. Cold-drawn pearlitic steel wires are the strongest structural bulk materials available with strength values above 6.4 GPa [8]. Such materials are used for applications such as suspension bridge cables, tire cords and springs. The cementite in this material dissociates upon plastic deformation [9–15] leading to enrichment of carbon in the ferrite. The material used in the present study was pearlitic steel wires with the chemical composition 0.81 C–0.20 Si–0.49 Mn–0.006 P–0.008 S (wt.%), provided by the Nippon Steel Corp. A detailed description of the fabrication is provided in Ref. [12]. During the process patented wires are produced by a well-defined thermo-mechanical treatment [12] which were subsequently cold drawn to true strains $\varepsilon = \ln(d_0^2/d^2)$ of 1.04, 1.97, 3.05, 3.98, and 5.01, respectively, where d is the final diameter of the wire.

* Corresponding author at: Institut für Materialphysik, Georg-August-Universität Göttingen, Friedrich-Hund-Platz 1, D-37077 Göttingen, Germany. Tel.: +49 551 39 5001; fax: +49 551 39 5000; e-mail addresses: rkirch@ump.gwdg.de; rkirch@material.physik.uni-goettingen.de

1359-6462/$ - see front matter © 2013 Acta Materialia Inc. Published by Elsevier Ltd. All rights reserved.
http://dx.doi.org/10.1016/j.scriptamat.2013.05.039

The temperature rise during deformation did not exceed 100 K [12].

Needle-shaped samples for APT measurements, termed tips, were prepared using a dual beam focused ion beam (FIB) FEI Nova NanoLab 600™. The tips were prepared perpendicular to the wire axis, since samples produced in this way were shown to be more reliable regarding the measured carbon concentration than samples prepared parallel to the wire axis [15,16]. In order to polish the surface and to reduce Ga implantation during the FIB process the upper atomic layers of the tips were removed by field evaporation using a field ion microscope. Then a thin Ni layer was deposited on the tip surface by ion beam sputter deposition. Additionally, a layer of Ag was deposited in order to stabilize the tip surface during APT measurements. Subsequently samples were heat treated at 423 K for 5–6 days and at 473 and 523 K for 8–24 h under vacuum at pressures of 10^{-5}–10^{-7} mbar. APT measurements were carried out at the Max-Planck-Institut für Eisenforschung using a LEAP 3000X HR™ and at the King Abdullah University of Science and Technology using a laser-assisted wide-angle tomographic atom probe (Cameca Instruments). Further APT measurements were performed at the Institut für Materialphysik in Göttingen using a conventional atom probe with a Cameca multi-anode detector.

In the present work the carbon concentration in ferrite was determined by analyzing APT measurements of pearlitic steel wires cold drawn to different true strains and after diffusion annealing treatments at temperatures between 473 and 523 K. The results are presented in Figure 1. For the as-patented wire ($\varepsilon = 0$) the carbon concentration in ferrite at room temperature was about 0.2 at.% and thus above the equilibrium concentration of carbon in ferrite (~0.01 at.%) and even higher than the values reported in previous APT measurements (0.05–0.07 at.%) [10,11,14]. The larger C concentrations in this study for $\varepsilon = 0$ may be caused by annealing the wires up to 473 K for interdiffusion to occur, whereas other studies analyzed wires after the patenting process without further annealing. The carbon content in ferrite remains approximately constant for $\varepsilon \leqslant 3$ and increases for $\varepsilon > 3$ up to about 0.6 at.% at $\varepsilon = 5.01$, which is three times that for the as-patented wire and in accord with Maruyama et al. [11]. In contrast, previous works showed an increase in the carbon concentration in ferrite even at low true strains caused by deformation-driven cementite decomposition [11,14]. A possible mechanism governing this decomposition process is the so-called "carbon drag effect" [17,18]. It proceeds by dislocations that move through the cementite lamellae and drag C atoms along with them because the binding energy between dislocations and C atoms in ferrite (0.75 eV [19]) is higher than the binding energy between carbon and iron atoms in cementite (0.40–0.42 eV [20,21]). Once drawn into the ferrite phase the C atoms then segregate to lattice defects, e.g. dislocations, vacancies, or (sub)-grain boundaries. Thus the carbon content in ferrite increases during deformation while it decreases in cementite [11,13,14]. The constant carbon concentration in ferrite determined in this work for $\varepsilon < 3$ is consistent with the observation that the cementite lamellae have a constant thickness of about 7–8 nm for $\varepsilon \leqslant 2$, while lamellae for $\varepsilon = 3$ and 5 have thicknesses of only 3 and 1–2 nm. Li et al. [14] observed cementite decomposition only for lamellae with a thickness of less than 8 nm for the same material. This indicates that cementite decomposition only starts at $\varepsilon \geqslant 3$ in the regions probed in our current samples, whereas the oversaturated carbon content at low true strains is probably influenced by our heat treatment after deformation. In contrast, sample annealing has no influence on the carbon concentration at higher deformations [8].

For samples with different true strains the Ni concentration profiles were determined perpendicular to the Ni–ferrite interfaces in regions where no cementite lamellae or grain boundaries were present. Thus any effect of the interfaces on Ni diffusion was avoided. The measured Ni and Fe concentrations observed after deposition of the Ni layer and after diffusion treatment are shown in Figure 2 as a function of the distance x from the Ni/ferrite interface. The concentration profile thickness where the concentration values change significantly was several nanometers. The corresponding extremely small diffusion lengths were at the lower limit of the resolution of APT. Thus precise calibration during APT reconstruction is required in order to obtain reliable values of the diffusion coefficient. In the case of the as-prepared Ni layer on the as-drawn sample the corresponding concentration profile was not step-like

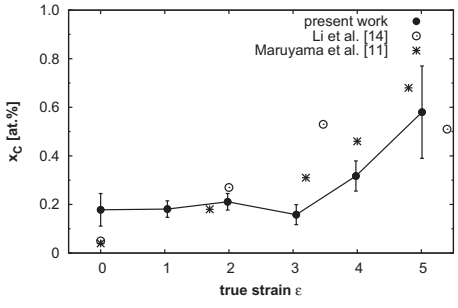

Fig. 1. Carbon concentration in ferrite in cold-drawn pearlitic wires after diffusion annealing at 473 K. For comparison APT results from the literature [11,14] are shown for as-patented ($\varepsilon = 0$) and as-drawn ($\varepsilon > 0$) wires without heat treatment. The error bars correspond to standard deviations from at least three measurements.

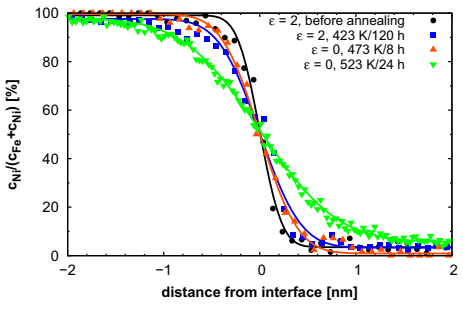

Fig. 2. Molar ratio of nickel plotted vs. the distance from the interface (defined by the 50% Ni isoconcentration surface) for the as-patented wire ($\varepsilon = 0$) after annealing at various temperatures and times, as shown in the inset. The lines are fits to Eq. (1).

(cf. Fig. 2), contradicting negligible diffusion. A step-like profile is absent because of the limited resolution of the atom probe and the initial roughness of the Ni/ferrite interface.

The Ni diffusion profiles were fitted to the error function erfc according to the equation [22]:

$$c_{Ni}/c_{Ni} + c_{Fe}(x) = (c_1 - c_2/2)\mathrm{erfc}(x/2\sqrt{D(t+t_v)}) + c_2 \quad (1)$$

where c_{Ni} and c_{Fe} are the measured nickel and iron concentrations, respectively, c_1 and c_2 are the initial nickel concentrations in the nickel and the ferrite phases, respectively, t is the annealing time and t_v is virtual time. The product Dt_v is obtained by fitting Eq. (1) to the initial profile of the as-prepared sample. After interdiffusion fitting the profiles yield $D(t + t_v)$, and by subtracting Dt_v the product Dt is obtained. The corresponding diffusion coefficients D were calculated from these fits for the data obtained on the annealed samples (lines in Fig. 2). For the annealing temperature 473 K the diffusion coefficients for different true strains are shown in Figure 3. The diffusion coefficient of the as-patented state ($\varepsilon = 0$) was calculated to be 10^{-24} m^2 s^{-1}, which is about seven orders of magnitude larger than the Ni impurity diffusion coefficient in α-Fe at the same temperature [6], but about 1.5 orders of magnitude below the grain boundary diffusion of Ni in α-Fe at 475 K [23]. In this work the selected volumes used to determine concentration profiles contained no grain boundaries and no cementite/ferrite interfaces. As observed for the carbon concentration, the diffusion coefficient remains approximately constant at a value of 1×10^{-24} m^2 s^{-1} for $\varepsilon \leqslant 3$. For $\varepsilon = 5.01$ the diffusion coefficient is about 1.5 times larger compared with the as-patented wire. The fact that Ni diffusion in ferrite for both the as patented and strained pearlite wires is much faster than Ni diffusion in bulk iron is attributed to vacancy–carbon complexes. These are formed, in addition to thermal vacancies, due to the attractive carbon–vacancy interaction. As shown by first-principles calculations [4,24–26], the increased total vacancy concentration leading to a higher diffusion coefficient arises from the reduced formation energy of vacancy–carbon complexes compared with carbon-free vacancies. At higher true strains, at which cementite decomposition occurred, the additional carbon atoms in ferrite form new complexes which lead to a higher vacancy concentration. This explains the strong correlation between carbon content and diffusion coefficient, as observed for other metals with carbon solute [1–3]. The diffusion coefficients of Ni in ferrite for the as-patented wire ($\varepsilon = 0$) were evaluated from various Ni concentration profiles, yielding values between 10^{-23} and 10^{-25} m^2 s^{-1} after annealing at 423–523 K. The averages and standard deviations of these values are shown in Figure 4 as an Arrhenius diagram. Fitting a straight line to the data in Figure 4 yields an activation energy of $Q = 0.66 \pm 0.05$ eV. However, the activation enthalpy Q in ferrite estimated in this work is based on a small number of measured values at only three different annealing temperatures. Thus the following interpretation regarding the quantitative aspects should be treated with some caution.As the interdiffusing elements Ni and Fe are rather similar, especially with respect to the size of their atoms, we assume that the diffusion coefficients D_i of iron and nickel are the same and equal to the interdiffusion coefficient $\tilde{D}$. This assumption is supported by the symmetric concentration profiles of both Ni and Fe. Furthermore, we assume that the thermodynamic factor which represents the influence of interaction between the different atoms is less dependent on temperature than the exponential term in D. Then the activation energy in $\tilde{D}$ is equal to the sum of the enthalpies h_V^f and h_V^m for vacancy formation and migration:

$$Q = R(\partial(\ln\tilde{D})/(\partial(1/T)) = h_V^f + h_V^m \quad (2)$$

In previous works the activation enthalpies of self-diffusion in pure α-Fe were mostly determined to be between 2.55 and 2.63 eV [7,27,28]. Values for the formation contribution h_V^f were estimated to be between 1.5 and 2.0 eV [29,30], whereas the contribution from migration h_V^m was 0.5–0.8 eV [5,31,32].

The activation energy determined in this study for Ni diffusion in ferrite was significantly smaller than the value for self-diffusion in α-Fe. A possible explanation for this result is given by the so-called defactant model developed by Kirchheim [33,34]. According to this model the C atoms present in ferrite segregate at vacancies and appreciably reduce the enthalpy of formation h_V^f of these defects, analogous to the reduction in surface

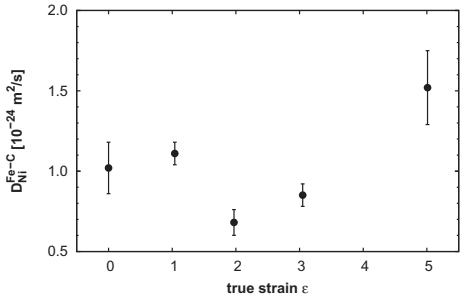

Fig. 3. Diffusion coefficient of Ni in ferrite ($\varepsilon = 0$) annealed at 473 K as a function of wire strain. The error bars are the standard deviations of the mean values.

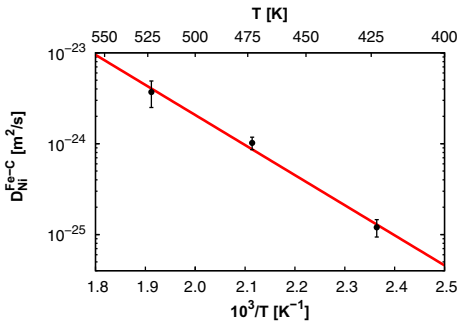

Fig. 4. Diffusion coefficient of Ni in ferrite ($\varepsilon = 0$) as a function of inverse annealing temperature. The error bars are the standard deviations of at least three measurements. The resulting linear regression function giving the activation enthalpy of diffusion is also shown.

energy of liquids due to the presence of "surfactant" molecules [35]. Facilitated vacancy formation by the formation of vacancy–carbon complexes leads to an increased vacancy concentration and thus to an enhanced diffusion coefficient. A detailed discussion of enhancement of the vacancy concentration in the presence of carbon solute within the framework of the defactant concept can be found in Kresse [36].

Previous works have also shown an influence of carbon on the vacancy migration enthalpy h_V^m, which is higher in carbon-enriched iron (0.73–1.3 eV [37,38]) compared with pure α-Fe. However, these enthalpies were determinated at temperatures above 580 K, when the vacancy–carbon complexes had already dissociated [31,39]. Furthermore, the activation enthalpy measured in this study is in the range of the vacancy migration enthalpy in pure iron, thus the influence of carbon on h_V^m in the temperature range of stable complexes is negligible. Under these conditions the measured activation energy of 0.66 eV represents the migration enthalpy of vacancy–carbon complexes. The reason why the enthalpy of vacancy formation makes no contribution despite Eq. (1) can be explained in two ways. First, the carbon concentration in ferrite is so high that the enthalpy of vacancy formation is reduced to zero within the framework of the defactant concept [33,34]. Second, sinks and sources of vacancies are insufficiently effective to establish thermodynamic equilibrium in the temperature range used in this study and, therefore, the concentration of vacancy–carbon complexes remains constant. In summary, the interdiffusion coefficients of Ni in ferrite at low temperatures were measured for pearlitic steel wires cold drawn to different true strains by APT. The measured values are six orders of magnitude larger than the Ni diffusion coefficient in bcc iron, which is attributed to an enhanced concentration of vacancies or, rather, vacancy–carbon complexes. Furthermore, the diffusion coefficient increases with higher carbon content, analogous to the results of previous studies on other metals with carbon solute [1,3]. The appreciably reduced activation enthalpy of interdiffusion can be explained by the defactant concept [33,34], explaining the pronounced reduction in vacancy formation enthalpy by oversaturated carbon solute or the high chemical potential of carbon, respectively.

The authors thank Prof. S. Goto of Akita University, Japan, and the Nippon Steel Corp. for fabrication and providing the cold-drawn specimens. We also thank U. Tezins of the Max-Planck-Institut für Eisenforschung in Düsseldorf for performing the LEAP measurements. We are grateful to the Deutsche Forschungsgemeinschaft for funding this Project (SFB 602, TP B13). T.A.-K. acknowledges the generous support of KAUST baseline funds.

[1] H.W. Mead, C.E. Birchenall, Trans. AIME 206 (1956) 1336.
[2] C. Köstler, F. Faupel, T. Hehenkamp, Scripta Mater. 20 (1986) 1755.
[3] D. Schmid. PhD thesis, University of Göttingen, 1990.
[4] M. Kabir, T.T. Lau, X. Lin, S. Yip, K.J. Van Vliet, Phys. Rev. B 82 (2010) 134112.
[5] C.C. Fu, E. Meslin, A. Barbu, F. Willaime, V. Oison, Solid State Phenom. 139 (2008) 157.
[6] K. Hirano, M. Cohen, B.L. Averbach, Acta Metall. 9 (1961) 440.
[7] F.S. Buffington, K. Hirano, M. Cohen, Acta Metall. 9 (1961) 434.
[8] Y.J. Li, P. Choi, S. Goto, C. Borchers, D. Raabe, R. Kirchheim, Acta Mater. 60 (2012) 4005.
[9] V.N. Gridnev, V.G. Gavrilyuk, I.Y. Dekhtyar, Y.Y. Meshkov, P.S. Nizin, Prokopenko, Phys. Status Solidi A 14 (1972) 689.
[10] M.H. Hong, W.T. Reynolds Jr., T. Tarui, K. Hono, Metall. Mater. Trans. A 30 (1999) 717.
[11] N. Maruyama, T. Tarui, H. Tashiro, Scripta Mater. 46 (2002) 599.
[12] S. Goto, R. Kirchheim, T. Al-Kassab, C. Borchers, Trans. Nonferrous Met. Soc. China 17 (2007) 1129.
[13] C. Borchers, T. Al-Kassab, S. Goto, R. Kirchheim, Mater. Sci. Eng., A 502 (2009) 131.
[14] Y.J. Li, P. Choi, C. Borchers, S. Westerkamp, S. Goto, D. Raabe, R. Kirchheim, Acta Mater. 59 (2011) 3965.
[15] Y.J. Li, P. Choi, C. Borchers, Y.Z. Chen, S. Goto, D. Raabe, R. Kirchheim, Ultramicroscopy 111 (2011) 628.
[16] J. Takahashi, T. Tarui, K. Kawakami, Ultramicroscopy 109 (2009) 193.
[17] V.N. Gridnev, V.V. Nemoshkalenko, Y.Y. Meshkov, V.G. Gavrilyuk, G. Prokopenko, O.N. Razumov, Phys. Status Solidi A 31 (1975) 201.
[18] V.G. Gavriljuk, Scr. Mater. 45 (2001) 1469.
[19] A.W. Cochardt, G. Schoek, H. Wiedersich, Acta Metall. 3 (1955) 533.
[20] R.A. Johnson, G.I. Diens, A.C. Damask, Acta Metall. 12 (1964) 125.
[21] R.A. Johnson, Acta Metall. 15 (1967) 513.
[22] P.G. Shewmon, Diffusion in Solids, second ed., McGraw Hill, New York, 1963.
[23] D. James, G. Leak, Phil. Mag. 12 (1965) 491.
[24] C. Domain, C.S. Becquart, Phys Rev B 65 (2001) 024103.
[25] C. Domain, C.S. Becquart, J. Foct, Phys. Rev. B 69 (2004) 144112.
[26] C.J. Forst, J. Slycke, K.J. Van Vliet, S. Yip, Phys. Rev. Lett. 96 (2006) 175501.
[27] R.B. McLellan, M.L. Wasz, Phys. Status Solidi A 110 (1988) 421.
[28] D.W. James, G.M. Leak, Phil. Mag. 14 (1966) 701.
[29] H.E. Schaefer, K. Maier, M. Weller, D. Herlach, A. Seeger, J. Diehl, Scr. Metall. 11 (1977) 803.
[30] L. De Schepper, G. Knuyt, L. Stals, D. Segers, L. Dorikens-Vanpraet, M. Dorikens, P. Moser, Mat. Sci. Forum 15–18 (1987) 131.
[31] A. Vehanen, P. Hautojärvi, J. Johansson, J. Yli-Kauppila, Phys. Rev. B 25 (1982) 762.
[32] G.J. Ackland, D.J. Bacon, A.F. Calder, T. Harry, Phil. Mag. A 75 (1997) 713.
[33] R. Kirchheim, Acta Mater. 55 (2007) 5129.
[34] R. Kirchheim, Acta Mater. 55 (2007) 5139.
[35] J.W. GibbsThe Collected Work of J.W., vol. 1, Longmans, Green & Co., New York, 1928, p. 55.
[36] T. Kresse, PhD thesis, University of Göttingen, 2013.
[37] T. Tabata, H. Fujita, H. Ishii, K. Igaki, M. Isshik, Scr. Metall. 15 (1981) 1317.
[38] A. Hardouin Duparc, C. Moingeon, N. Smetniansky-de-Grande, A. Barbu, J. Nucl. Mater. 302 (2002) 143.
[39] S. Takaki, J. Fuss, H. Kugler, U. Dedek, H. Schultz, Rad. Eff. 79 (1983) 87.